

## The effect of core polarization on longitudinal form factors in $^{10}\text{B}$

This article has been downloaded from IOPscience. Please scroll down to see the full text article.

2012 Phys. Scr. 85 065201

(<http://iopscience.iop.org/1402-4896/85/6/065201>)

View [the table of contents for this issue](#), or go to the [journal homepage](#) for more

Download details:

IP Address: 93.187.33.97

The article was downloaded on 09/05/2012 at 04:53

Please note that [terms and conditions apply](#).

# The effect of core polarization on longitudinal form factors in $^{10}\text{B}$

Fouad A Majeed

Department of Physics, College of Education for Pure Science, University of Babylon, PO Box 4, Hilla-Babylon, Iraq

E-mail: [fouadalajeeli@yahoo.com](mailto:fouadalajeeli@yahoo.com)

Received 20 February 2012

Accepted for publication 16 April 2012

Published 8 May 2012

Online at [stacks.iop.org/PhysScr/85/065201](http://stacks.iop.org/PhysScr/85/065201)

## Abstract

Electron scattering Coulomb form factors for the single-particle quadrupole transitions in the p-shell  $^{10}\text{B}$  nucleus have been studied. Core polarization effects are included through a microscopic theory that includes excitations from the core orbits up to higher orbits with  $2\hbar\omega$  excitations. The modified surface delta interaction is employed as a residual interaction. The effect of core polarization is found essential in both the transition strengths and momentum transfer dependence of form factors, and gives remarkably good agreement with the measured data with no adjustable parameters.

PACS numbers: 25.30.Dh, 21.60.Cs, 27.20.+n

## 1. Introduction

Comparisons between calculated and measured longitudinal electron scattering form factors have long been used as stringent tests of models of nuclear structure [1, 2]. Shell model within a restricted model space succeeded in describing static properties of nuclei when effective charges are used. The Coulomb form factors have been discussed for the stable sd-shell nuclei using sd-shell wave functions with phenomenological effective charges [3]. For p-shell nuclei, the Cohen–Kurath (CK) [4] model explains the low-energy properties of p-shell nuclei well. However, at higher-momentum transfer, it fails to describe the form factors. Radhi *et al* [5–9] have successfully proved that the inclusion of core polarization (CP) effects in the p-shell and sd-shell is essential to improve the calculations of the form factors. Restricted 1p-shell models were found to provide good predictions for the  $^{10}\text{B}$  natural parity level spectrum and transverse form factors [10]. However, they were less successful for  $C2$  form factors and give just 45% of the total observed  $C2$  transition strength. Expanding the shell-model space to include  $2\hbar\omega$  configurations in describing the form factors of  $^{10}\text{B}$ , Cichocki *et al* [10] found that only a 10% improvement was realized. The purpose of this work is to study the  $C2$  form factors for  $^{10}\text{B}$  by including higher-energy configurations as a first-order CP through a microscopic theory, which combines shell model wave functions and highly excited states. Single-particle wave functions are used

as a zeroth contribution and the effect of CP is included as a first-order perturbation theory with the modified surface delta interaction (MSDI) [11] as a residual interaction and a  $2\hbar\omega$  for the energy denominator. The single-particle wave functions are those of the harmonic-oscillator (HO) potential with size parameter  $b$  chosen to reproduce the measured root-mean-square (rms) charge radii of these nuclei.

## 2. Theory

The CP effect on the form factors is based on a microscopic theory, which combines shell model wave functions and configurations with higher energy as first-order perturbations; these are called CP effects. The reduced matrix elements of the electron scattering operator  $T_\Lambda$  are expressed as the sum of the product of the elements of the one-body density matrix (OBDM)  $\chi_{\Gamma_f\Gamma_i}^\Lambda(\alpha, \beta)$  times the single-particle matrix elements, and are given by

$$\langle \Gamma_f ||| T_\Lambda ||| \Gamma_i \rangle = \sum_{\alpha, \beta} \chi_{\Gamma_f\Gamma_i}^\Lambda(\alpha, \beta) (\alpha ||| T_\Lambda ||| \beta), \quad (1)$$

where  $\alpha$  and  $\beta$  label single-particle states (isospin is included) for the model space. For p-shell nuclei, the orbits  $1p_{3/2}$  and  $1p_{1/2}$  define the model space. The states  $|\Gamma_i\rangle$  and  $\Gamma_f$  are described by the model space wave functions. Greek symbols are used to denote quantum numbers in the coordinate space and isospace, i.e.  $\Gamma_i \equiv J_i T_i$ ,  $\Gamma_f \equiv J_f T_f$  and

$\Lambda = JT$ . According to the first-order perturbation theory, the single-particle matrix element is given by [11]

$$\begin{aligned} \langle \alpha ||| T_\Lambda ||| \beta \rangle &= \langle \alpha ||| T_\Lambda ||| \beta \rangle + \left\langle \alpha ||| T_\Lambda \frac{Q}{E_i - H_0} V_{\text{res}} ||| \beta \right\rangle \\ &+ \left\langle \alpha ||| V_{\text{res}} \frac{Q}{E_f - H_0} T_\Lambda ||| \beta \right\rangle. \end{aligned} \quad (2)$$

The first term is the zeroth-order contribution. The second and third terms are the CP contributions. The operator  $Q$  is the projection operator onto the space outside the model space. For the residual interaction,  $V_{\text{res}}$ , we adopt the MSDI [11].  $E_i$  and  $E_f$  are the energies of the initial and final states, respectively. The CP terms are written as [11]

$$\begin{aligned} \sum_{\alpha_1, \alpha_2, \Gamma} \frac{(-1)^{\beta + \alpha_2 + \Gamma}}{e_\beta - e_\alpha - e_{\alpha_1} + e_{\alpha_2}} (2\Gamma + 1) \begin{Bmatrix} \alpha & \beta & \Lambda \\ \alpha_2 & \alpha_1 & \Gamma \end{Bmatrix} \\ \times \sqrt{(1 + \delta_{\alpha_1 \alpha}) (1 + \delta_{\alpha_2 \beta})} \langle \alpha \alpha_1 | V_{\text{res}} | \beta \alpha_2 \rangle \langle \alpha_2 ||| T_\Lambda ||| \alpha_1 \rangle \\ + \text{terms with } \alpha_1 \text{ and } \alpha_2 \text{ exchanged with an overall minus sign,} \end{aligned} \quad (3)$$

where the indices  $\alpha_1$  and  $\alpha_2$  run over particle states and  $e$  is the single-particle energy. The CP parts are calculated by keeping the intermediate states up to the 2p1f-shells. The single-particle matrix element reduced in both spin and isospin is written in terms of the single-particle matrix element reduced in spin only [11]:

$$\langle \alpha_2 ||| T_\Lambda ||| \alpha_1 \rangle = \sqrt{\frac{2T+1}{2}} \sum_{t_z} I_T(t_z) \langle \alpha_2 || T_\Lambda || \alpha_1 \rangle \quad (4)$$

with

$$I_T(t_z) = \begin{cases} 1, & \text{for } T = 0 \\ (-1)^{1/2 - t_z}, & \text{for } T = 1 \end{cases}, \quad (5)$$

where  $t_z = 1/2$  for protons and  $-1/2$  for neutrons. The reduced single-particle matrix element of the Coulomb operator is given by [12]

$$\langle \alpha_2 ||| T_J ||| \alpha_1 \rangle = \int_0^\infty dr r^2 j_J(qr) \langle \alpha_2 || Y_J || \alpha_1 \rangle R_{n_1 \ell_1} R_{n_2 \ell_2}, \quad (6)$$

where  $j_J(qr)$  is the spherical Bessel function and  $R_{n\ell}(r)$  is the single-particle wave function. The electron scattering form factor involving angular momentum  $J$  and momentum transfer  $q$ , between the initial and final nuclear shell model states of spin  $J_{i,f}$  and isospin  $T_{i,f}$ , is [13]

$$\begin{aligned} |F_J(q)|^2 &= \frac{4\pi}{Z^2(2J_i + 1)} \left| \sum_{T=0,1} \begin{pmatrix} T_f & T & T_i \\ -T_z & 0 & T_z \end{pmatrix} \right|^2 \\ &\times |\langle \alpha_2 ||| T_\Lambda ||| \alpha_1 \rangle|^2 |F_{c.m.}(q)|^2 |F_{f.s.}(q)|^2, \end{aligned} \quad (7)$$

where  $T_z$  is the projection along the  $z$ -axis of the initial and final isospin states and is given by  $T_z = (Z - N)/2$ . The nucleon finite-size (f.s) form factor is  $F_{f.s.}(q) = \exp(-0.43q^2/4)$  and  $F_{c.m.}(q) = \exp(q^2 b^2/4A)$  is a correction for the lack of translational invariance in the shell model.

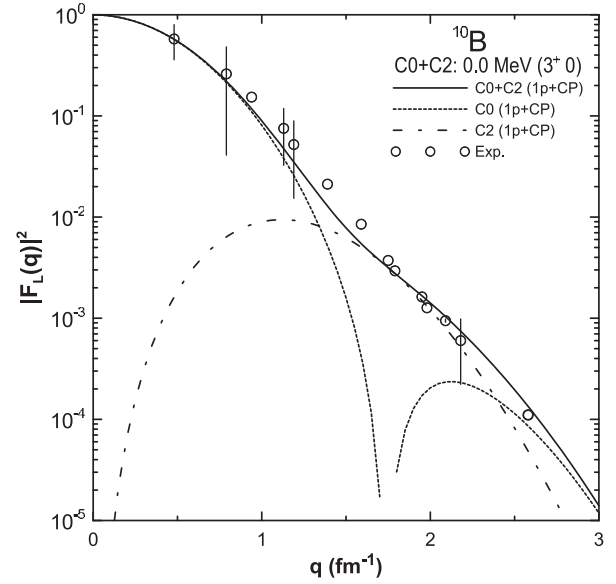


**Figure 1.** The longitudinal C0+C2 form factor for the isoscalar  $3^+_{g.s.}$  (0.0 MeV) transition in  $^{10}\text{B}$  compared with the experimental data taken from [10].

$A$  is the mass number and  $b$  is the HO size parameter. The single-particle energies are calculated according to [11]

$$\begin{aligned} e_{nlj} &= (2n + l - 1/2)\hbar\omega \\ &+ \begin{cases} -\frac{1}{2}(l+1)\langle f(r) \rangle_{nl} & \text{for } j = l - 1/2 \\ \frac{1}{2}l\langle f(r) \rangle_{nl} & \text{for } j = l + 1/2 \end{cases}, \end{aligned} \quad (8)$$

with  $\langle f(r) \rangle_{nl} \approx -20A^{-2/3}$  and  $\hbar\omega = 45A^{-1/3} - 25A^{-2/3}$ . The electric transition strength is given by [11]

$$B(CJ, k) = \frac{Z^2}{4\pi} \left[ \frac{(2J+1)!!}{k^J} \right]^2 F_J^2(k), \quad (9)$$

where  $k = E_x/\hbar c$ .

### 3. Results and discussion

The CP effects are calculated with the MSDI as a residual interaction. The parameters of the MSDI are denoted by  $A_T$ ,  $B$  and  $C$  [11], where  $T$  indicates the isospin (0,1). These parameters are taken to be  $A_0 = A_1 = B = 25/A$  and  $C = 0$ , where  $A$  is the mass number. In all of the following diagrams (see figure 1), the dashed lines give the results obtained using the 1p-shell wave functions (1p) of the Cohen–Kurath two-body matrix element interaction (CK-TBME) [4]. The results of the CP effects are shown by dashed-dotted lines. The results including core polarization (1p+CP) are shown by solid lines. The  $B(C2 \uparrow, q)$  values as a function of momentum transfer  $q$  are achieved by removing from the form factors most of the dependence on the momentum transfer, according to the transformation given in [3]. The  $B(C2 \uparrow)$  values are given at the photon point defined at  $q = k = E_x/\hbar c$ , and are displayed in table 1. The size parameter  $b$  is taken to be 1.71 fm [14] to obtain the single-particle wave functions of the HO potential.

The calculations for the C0 and C2 isoscalar transition from the ground state ( $J_i^\pi = 3^+, T = 0$ ) to the ground state

**Table 1.** Theoretical values of the reduced transition probabilities  $B(C2 \uparrow, q)$  (in units of  $e^2 \text{fm}^4$ ) in comparison with the experimental values and other theoretical calculations for  $^{10}\text{B}$ .

$J_f^\pi$	$T_f$	$E_x(\text{MeV})$	$b$ (fm)		Other	Expt.	
			[14]	1p	1p+CP	[10]	[10]
$3_1^+$	0	0.000	1.71				
$1^+$	0	0.718	1.71	0.889	1.77	1.62	$1.7 \pm 0.3$
$2^+$	0	3.587	1.71	0.568	1.55	1.36	$0.6 \pm 0.1$
$3_2^+$	0	4.774	1.71	0.56	1.66	1.63	$< 0.04$
$4^+$	0	6.025	1.71	5.79	11.67	11.74	$17.4 \pm 0.7$

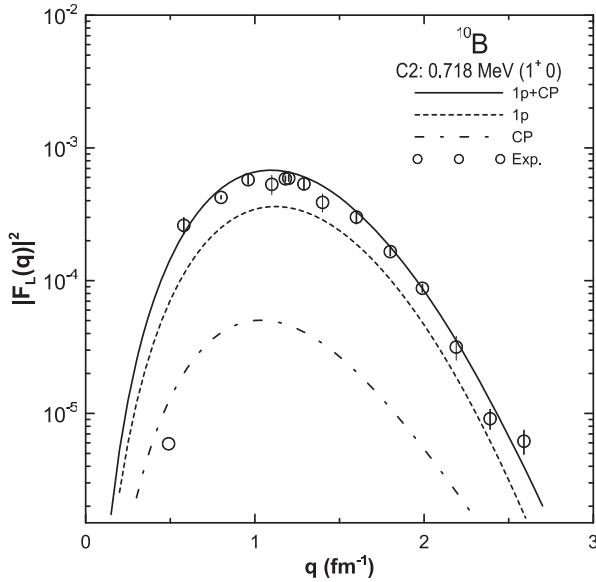
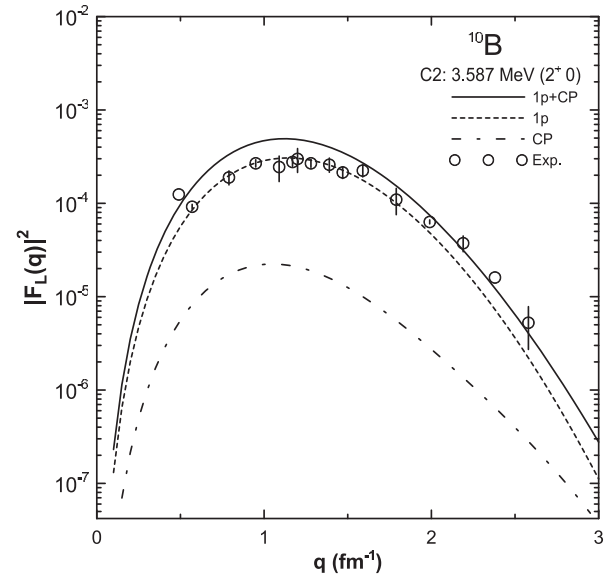


**Figure 2.** The longitudinal  $C2$  form factor for the isoscalar  $1^+$  (0.718 MeV) transition in  $^{10}\text{B}$  compared with the experimental data taken from [10].

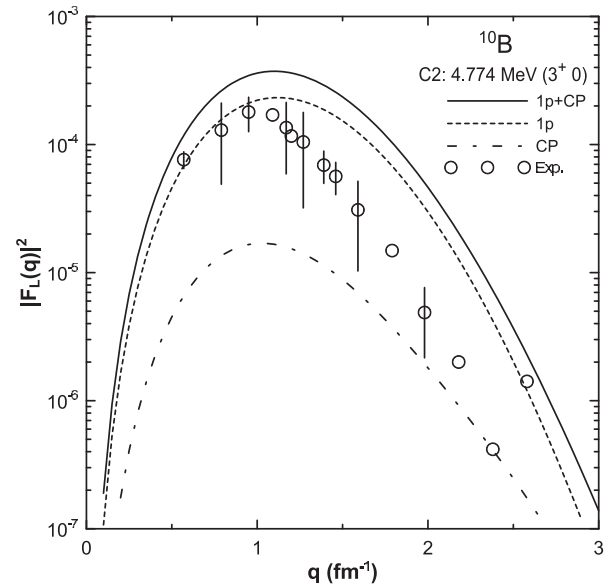
( $J_f^\pi = 3^+$ ,  $T = 0$ ) at  $E_x = 0.0 \text{ MeV}$  are shown in figure 1. The multipole decomposition is displayed as indicated by  $C0$  and  $C2$ . The total form factor is shown by the solid curve, where the data are described well in all the momentum transfer regions up to  $q \leq 2.58 \text{ fm}^{-1}$ . The CP effects enhance the  $C2$  form factor appreciably by a factor of around 2 over the 1p-shell calculation. This enhancement brings the total form factor (solid curve) very close to the experimental data. Similar results are obtained in [10].

Figure 2 displays the calculation of the  $C2$  form factor to the ( $J_f^\pi = 1^+$ ,  $T = 0$ ) at  $E_x = 0.718 \text{ MeV}$ . The 1p-shell model calculation underestimates the experiment and the inclusion of the CP enhances the calculations and brings the form factor to the experimental values in all momentum transfer regions. The result of the 1p-shell model calculations predicts the  $B(C2 \uparrow)$  value to be  $0.889 e^2 \text{fm}^4$  in comparison with the measured value  $1.7 \pm 0.3 e^2 \text{fm}^4$  [10]. Inclusion of the CP effect predicts the value to be  $1.77 e^2 \text{fm}^4$ , which is very close to the measured value and those given in previous theoretical works [5, 10] as shown in table 1.

The  $C2$  form factor for the ( $J_f^\pi T_f = 2^+0$ ) at  $E_x = 3.587 \text{ MeV}$  is shown in figure 3; the 1p-shell model calculations describe the experimental data very well up to momentum transfer  $q \leq 2.0 \text{ fm}^{-1}$  where they start to deviate from the experiment. The inclusion of the CP effect overestimates the measured form factors up to  $q \sim 2.0 \text{ fm}^{-1}$  and comes to the measured form factors at  $q \sim (2-3) \text{ fm}^{-1}$ .



**Figure 3.** The longitudinal  $C2$  form factor for the isoscalar  $2^+$  (3.587 MeV) transition in  $^{10}\text{B}$  compared with the experimental data taken from [10].



**Figure 4.** The longitudinal  $C2$  form factor for the isoscalar  $3^+$  (4.774 MeV) transition in  $^{10}\text{B}$  compared with the experimental data taken from [10].

The calculated  $B(C2 \uparrow)$  value is found to be equal to  $0.568 e^2 \text{fm}^4$  (without CP) and  $1.55 e^2 \text{fm}^4$  (with CP) in comparison with the measured value  $0.6 \pm 0.1 e^2 \text{fm}^4$  [10] as displayed in table 1.

Figure 4 shows the comparison of the calculated longitudinal  $C2$  form factors from the ground state ( $J_i^\pi = 3_1^+$ ,  $T = 0$ ) to the excited state ( $J_f^\pi = 3_2^+$ ,  $T = 0$ ) at  $E_x = 4.774 \text{ MeV}$ . The 1p-shell model calculations reproduce the low- $q$  values up to  $q \leq 1.0 \text{ fm}^{-1}$  where they start to deviate severely and the inclusion of the CP effects makes the calculation worse and brings it higher than the 1p calculation. Our calculations are consistent with those of [10], and in order to fit the measured form factor, the authors adopted the harmonic oscillator wave function with size parameter

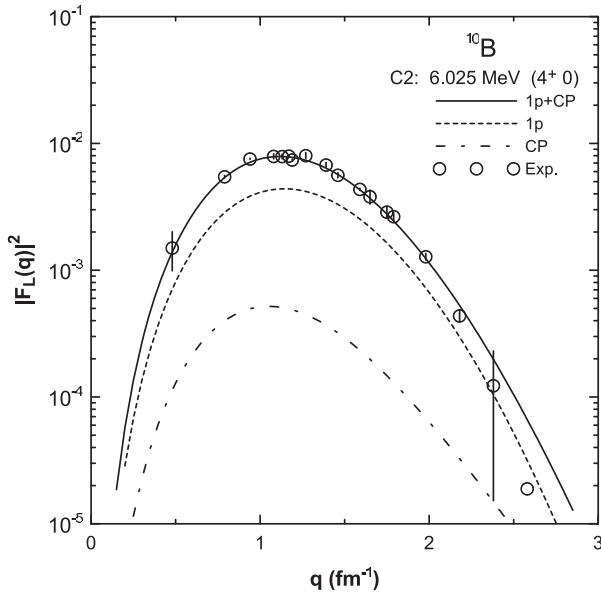


**Figure 5.** The longitudinal  $C2$  form factor for the isoscalar  $4^+$  ( $3.587$  MeV) transition in  $^{10}\text{B}$  compared with the experimental data taken from [10].

$b = 1.5$  fm to calculate the  $8.66$  MeV  $C0$  form factor in  $^{13}\text{C}$ , and they normalized it to fit the  $4.774$  MeV  $^{10}\text{B}$  data. The comparison of the calculated  $B(C2 \uparrow)$  is found to be  $0.56 e^2\text{fm}^4$  with  $1p$  and  $1.66 e^2\text{fm}^4$  with  $1p+CP$ , in comparison with the measured value  $< 0.04, e^2\text{fm}^4$  [10].

The longitudinal  $C2$  form factor for the transition ( $J^\pi = 4^+, T = 0$ ) state at  $E_x = 6.025$  MeV is shown in figure 5; the inclusion of the CP effects improves the calculations of the  $C2$  form factor and brings them to the experimental values in all momentum transfer regions. The calculation of  $B(C2 \uparrow)$  with  $1p$  is found to be  $5.79 e^2\text{fm}^4$ , while with  $1p+CP$  it is  $11.67 e^2\text{fm}^4$  in comparison with the measured value  $17.4 \pm 0.7 e^2\text{fm}^4$  [10] as shown in table 1. It is very clear that the  $1p$ -shell model fails to describe the data in both the transition strength ( $B(C2 \uparrow) = 5.79 e^2\text{fm}^4$ ) and the form factors. The inclusion of CP effects gives

remarkably good agreement with the experimental data in all regions of the momentum transfers  $q$  and enhances the result by a factor of 3 over the  $1p$ -shell model results.

#### 4. Conclusions

The  $1p$ -shell models, which can describe static properties and energy levels, are less successful in describing dynamic properties such as  $C2$  transition rates and electron scattering form factors. The average underestimation of the  $B(C2 \uparrow)$  value from the experiment is about a factor of 2. The inclusion of higher-excited configurations by means of CP enhances the form factors and brings the theoretical results closer to the experimental data. The average  $B(C2 \uparrow)$  value becomes about 90% of the average experimental value when CP effects are included, for the transitions considered in this work. All calculations presented in this work have been performed by employing MSDI as the residual interaction. The use of modern effective interaction may give a better description of the form factors.

#### References

- [1] Majeed F A 2007 *Phys. Scr.* **76** 332
- [2] Majeed F A and Radhi R A 2006 *Chin. Phys. Lett.* **23** 2699
- [3] Brown B A, Radhi R and Wildenthal B H 1983 *Phys. Rep.* **101** 313
- [4] Cohen S and Kurath D 1965 *Nucl. Phys.* **73** 1
- [5] Radhi R A, Abdullah A A, Dakhil Z A and Adeeb N M 2001 *Nucl. Phys. A* **696** 442
- [6] Radhi R A 2002 *Nucl. Phys. A* **707** 56
- [7] Radhi R A 2003 *Eur. Phys. J. A* **16** 381
- [8] Radhi R A 2002 *Nucl. Phys. A* **716** 100
- [9] Radhi R A 2003 *Eur. Phys. J. A* **16** 381
- [10] Cichocki A, Dubach J, Hicks R S, Peterson G A, de Jager C W, de Vries H, Kalantar-Nayestanaki N and Sato T 1995 *Phys. Rev. C* **51** 2406
- [11] Brussaard P J and Glaudemans P W M 1977 *Shell-Model Applications in Nuclear Spectroscopy* (Amsterdam: North-Holland)
- [12] de Forest T Jr and Walecka J D 1966 *Adv. Phys.* **15** 1
- [13] Donnelly T W and Sick I 1984 *Rev. Mod. Phys.* **56** 461
- [14] de Vries H *et al* 1987 *At. Data Nucl. Data Tables* **495** 36